J|A|C|S
ARTICLES
Published on Web 02/21/2007

Efficient and Color-Tunable Mn-Doped ZnSe Nanocrystal Emitters: Control of Optical Performance via Greener Synthetic Chemistry

Narayan Pradhan and Xiaogang Peng*

Contribution from the Department of Chemistry & Biochemistry, University of Arkansas, Fayetteville, Arkansas 72701

Received November 21, 2006; E-mail: xpeng@uark.edu

Abstract: Formation of Mn-doped ZnSe quantum dots (Mn:ZnSe d-dots) using nucleation-doping strategy was studied *s*ystematically and optimized through greener approaches. The resulting d-dots were with high (~50%) photoluminescence (PL) quantum yield (QY), which was achieved by the controlled formation of small-sized MnSe nanoclusters as the core and a diffused interface between the nanocluster core and the ZnSe overcoating layers. Synthesis of the d-dots under high temperatures (240−300 °C) was achieved by varying the structure of the metal carboxylate precursors, concentration of the inhibitors, free fatty acid, and concentration of the activation reagents, fatty amines. Highly emissive d-dots synthesized under desired conditions were found to be extremely stable upon thermal treatment up to the boiling point of the solvent (about 300 °C), which was quantitatively studied using in situ measurements. The PL peak of the d-dots was controllably tuned in a surprisingly large optical window, from 565 to 610 nm. These highly emissive and stable d-dots possess characteristics of practical emissive materials, especially for applications requiring high power, high concentration of emitters, and under tough conditions.

Introduction

Doped semiconductor nanocrystals (d-dots), specifically ones not containing heavy metal ions, have the potential to become a class of mainstream emissive materials. As illustrated recently,[1] Mn- and Cu-doped ZnSe (Mn:ZnSe and Cu:ZnSe) d-dots can cover an emission window similar to that of the current workhorse of intrinsic quantum dot (q-dots) emitters, CdSe nanocrystals.[2,3] Besides their low toxicity by replacing cadmium in CdSe quantum dots with zinc, d-dot emitters can also overcome a couple of intrinsic disadvantages of undoped quantum dot emitters, that is, strong self-quenching caused by their small ensemble Stokes shift (energy difference between absorption spectrum and emission band)[4,5] and sensitivity to thermal, chemical, and photochemical disturbances.[1,6,7] These two intrinsic properties of undoped quantum dots may make them not ideal for several potential applications being actively pursued in the field, such as LEDs,[8] lasers,[9] solid-state lighting,[10] beads-based bar-coding,[11] and others requiring significant power and/or high density of nanocrystals.

As compared to common emissive materials, organic dyes and inorganic phosphor powders, undoped q-dot emitters possess apparent advantages, such as narrow and symmetric emission with tunable colors, broad and strong absorption, zero scattering, reasonable stability, and solution processibility. d-Dot emitters can potentially retain more or less all of these advantages. They overcome the self-quenching problems of undoped q-dots by their substantial ensemble Stokes shift. This large Stokes shift in d-dots was due to their relatively small emission energy gap, in comparison to the absorption band gap of the host nanocrystals, in their atomic-like emission states. These atomic-like states are inner core electronic states of the dopant centers, which thus do not couple to the lattice phonons strongly. Consequently, the emission of d-dots can be thermally stable.[12] For these reasons, d-dots may become a new class of practical emissive materials, which complement organic dyes, inorganic phosphors, and undoped q-dots.

Doped semiconductor nanocrystals are not new to the field. Many different synthetic approaches have been reported[13−24]

(1) Pradhan, N.; Goorskey, D.; Thessing, J.; Peng, X. *J. Am. Chem. Soc.* **2005**, *127*, 17586−17587.
(2) Murray, C. B.; Norris, D. J.; Bawendi, M. G. *J. Am. Chem. Soc.* **1993**, *115*, 8706−15.
(3) Hines, M. A.; Guyot-Sionnest, P. *J. Phys. Chem.* **1996**, *100*, 468−71.
(4) Kagan, C. R.; Murray, C. B.; Nirmal, M.; Bawendi, M. G. *Phys. Rev. Lett.* **1996**, *76*, 1517−20.
(5) Achermann, M.; Petruska, M. A.; Crooker, S. A.; Klimov, V. I. *J. Phys. Chem. B* **2003**, *107*, 13782−13787.
(6) Empedocles, S. A.; Norris, D. J.; Bawendi, M. G. *Phys. Rev. Lett.* **1996**, *77*, 3873−3876.
(7) Li, J. J.; Wang, Y. A.; Guo, W.; Keay, J. C.; Mishima, T. D.; Johnson, M. B.; Peng, X. *J. Am. Chem. Soc.* **2003**, *125*, 12567−12575.
(8) Colvin, V. L.; Schlamp, M. C.; Allvisatos, A. P. *Nature* **1994**, *370*, 354−7.
(9) Klimov, V. I.; Mikhailovsky, A. A.; Xu, S.; Malko, A.; Hollingsworth, J. A.; Leatherdale, C. A.; Eisler, H.; Bawendi, M. G. *Science* **2000**, *290*, 314−7.
(10) Lee, J.; Sundar, V. C.; Heine, J. R.; Bawendi, M. G. *Adv. Mater.* **2000**, *12*, 1102−1105.
(11) Han, M.; Gao, X.; Su, J. Z.; Nie, S. *Nat. Biotechnol.* **2001**, *19*, 631−635.
(12) Kim, J. H.; Holloway, P. H. *Adv. Mater.* **2005**, *17*, 91−96.
(13) Bhargava, R. N.; Gallagher, D.; Hong, X.; Nurmikko, A. *Phys. Rev. Lett.* **1994**, *72*, 416−19.
(14) Sooklal, K.; Cullum, B. S.; Angel, S. M.; Murphy, C. J. *J. Phys. Chem.* **1996**, *100*, 4551−5.
(15) St. John, J.; Coffer, J. L.; Chen, Y.; Pinizzotto, R. F. *J. Am. Chem. Soc.* **1999**, *121*, 1888−1892.
(16) Mikulec, F. V.; Kuno, M.; Bennati, M.; Hall, D. A.; Griffin, R. G.; Bawendi, M. G. *J. Am. Chem. Soc.* **2000**, *122*, 2532−2540.

10.1021/ja068360v CCC: $37.00

for developing doped emissive materials as well as other types of functional materials, such as dilute magnetic doped semiconductor materials.[25] The traditional synthetic approaches have been generally based on a reaction system with both dopant ions and competitive host ions in it, which is difficult to control and optimize. As a result, the resulting d-dots are often mixed with a significant portion of undoped nanocrystals, judged by their emission spectra. This situation was substantially improved by our recent report,[1] which reported tunable and pure dopant emission (>99% in intensity) from about 470 to 590 nm with PL QY around 10−30%. The key feature of the related synthetic chemistry is decoupling the doping from nucleation and/or growth through nucleation-doping and growth-doping strategies.[1] This allows, in principle, the placement of the dopant ions at a desired radial position in the host nanocrystals. During the preparation of this Article, we noticed that Cao's group[26] realized decoupling doping from nucleation and growth by isolating CdS core nanocrystals prior to the doping process. Although cadmium was still included in the resulting Mn-doped CdS/ZnS core/shell structure and might not be ideal for practical applications, the PL QY of their doped nanostructures was impressive, as high as 50%. From a synthetic point of view, their method is somewhat similar to the growth-doping strategy.

The potential of the new synthetic strategies, nucleation-doping and growth-doping, seems to be promising. However, several fundamental properties of the resulting d-dots need to be greatly improved for practical applications, such as PL QY, color tunability, color purity (emission peak width), surface/ligand chemistry, durability and stability, etc. For the nucleation-doping strategy to be discussed here, both energy transfer and emission processes should occur at the interface of the nuclei with the dopant ions as the emission centers and the pure host overcoating layer as the absorption zone. For this reason, the primary emphasis in this work was the controlled formation of the dopant-containing nuclei as well as the interface between the doped core and pure host shell. The surprising tunability of the emission wavelength of Mn:ZnSe d-dots observed previously was also studied further in this work. Overall, the synthetic schemes were developed with consideration of possible greener methods, that is, simpler, less time-consuming, and less dangerous than that reported previously.[1] A separate report[27] will deal with chemical and photochemical stability, biocompatibility, and bioaccessibility of these highly efficient d-dot emitters for biomedical applications. Although the current report concentrates on key issues of synthetic chemistry, some structural characterization of the resulting d-dots will also be provided and discussed.

Results

Control of the size of the MnSe core is the first key issue for the nucleation-doping process. Ideally, a small-sized nucleus would place the dopant ions as close as possible to the center of the d-dots. This shall result in emission centers as far away as possible from the potential surface trap states of the nanocrystals, and thus improve the optical performance of the d-dots. A small nucleus also means a relatively uniform environment of the doping ions in a d-dot. Furthermore, a small-sized nucleus might be more suited for formation of a better interface between the MnSe core and ZnSe shell, even a mutually diffused interface, in comparison to a large-sized MnSe nanocrystal. The latter hypothesis is based on the fact that the chemical potential of particles increases dramatically as their size decreases in the few nanometer size range.[28] A more practical issue needed to be addressed in this section is the slow formation rate (a few hours) of MnSe nuclei reported in the previous communication.[1]

One structural feature for the targeted d-dots is that the anionic precursor, specifically the Se precursor, is common for both host growth and nucleation. This offers a convenient handle for tuning the reaction conditions. In principle, if the Se precursor is used in large excess, the cationic precursor, Mn fatty acid salts, should be consumed rapidly, and small-sized MnSe nanoclusters would be the resulting products. Such small MnSe nanoclusters should be stable in the reaction solution because of the existence of an excessively high Se monomer concentration in the solution.[29]

When the precursor ratio was relatively low, formation of large-sized MnSe nanocrystals by continuous growth was observed. For the example in Figure 1a (Mn to Se precursor equals 1:8), the absorption edge gradually shifted to over 400 nm, which is similar to what was observed in the previous communication for MnSe particles larger than 4 nm in size.[1] When the Mn to Se precursor was 1:32 (Figure 1b), however, the absorption edge of the MnSe clusters stayed below 300 nm even after the reaction mixture was heated for about 1 h. The corresponding FTIR spectra (Figure 1c) revealed that Mn carboxylate was consumed within about 2 min, indicated by the disappearance of the asymmetric vibration peak of the $-COO^-$ group at about 1550 cm^{-1} (Figure 1c). Here, the IR peaks for the −C═C− double bond of octadecene as the solvent (labeled in Figure 1c) were used as the internal references.

Practically, the Se to Mn precursor ratio between 25:1 and 35:1 was found to be adequate for the formation of small and stable MnSe clusters. When this ratio was higher than 35, the large excess of Se precursor might cause some complication in the subsequent overcoating stage.

The quality of the Mn fatty acid salt precursor, such as Mn stearate ($MnSt_2$), played a determining role for the reproducibility of the synthesis. If a stoichiometric amount of base was mixed with the fatty acid prior to the addition of $MnCl_2$, the resulting $MnSt_2$ (after purification and drying) should be a white powder. If the reaction was with excess base, or the base was added after the mixing of the fatty acid and $MnCl_2$, the resulting fatty acid salts would be brownish (see Supporting Information,

(17) Norris, D. J.; Yao, N.; Charnock, F. T.; Kennedy, T. A. *Nano Lett.* **2001**, *1*, 3−7.
(18) Bol, A. A.; Meijerink, A. *J. Phys. Chem. B* **2001**, *105*, 10203−10209.
(19) Azad Malik, M.; O'Brien, P.; Revaprasadu, N. *J. Mater. Chem.* **2001**, *11*, 2382−2386.
(20) Radovanovic, P. V.; Norberg, N. S.; McNally, K. E.; Gamelin, D. R. *J. Am. Chem. Soc.* **2002**, *124*, 15192−15193.
(21) Raola, O. E.; Strouse, G. F. *Nano Lett.* **2002**, *2*, 1443−1447.
(22) Schwartz, D. A.; Norberg, N. S.; Nguyen, Q. P.; Parker, J. M.; Gamelin, D. R. *J. Am. Chem. Soc.* **2003**, *125*, 13205−13218.
(23) Yang, H.; Santra, S.; Holloway, P. H. *J. Nanosci. Nanotechnol.* **2005**, *5*, 1364−75.
(24) Erwin, S. C.; Zu, L.; Haftel, M. I.; Efros, A. L.; Kennedy, T. A.; Norris, D. J. *Nature* **2005**, *436*, 91−94.
(25) Radovanovic, P. V.; Gamelin, D. R. *J. Am. Chem. Soc.* **2001**, *123*, 12207−12214.
(26) Yang, Y.; Chen, O.; Angerhofer, A.; Cao, Y. C. *J. Am. Chem. Soc.* **2006**, *128*, 12428−12429.
(27) Pradhan, N.; Battaglia, D.; Liu, Y.; Peng, X. *Nano Lett.* **2006**, ASAP, DOI: 10.1021/nI062336y.
(28) Peng, X. *Chem.-Eur. J.* **2002**, *8*, 334−339.
(29) Peng, X.; Wickham, J.; Alivisatos, A. P. *J. Am. Chem. Soc.* **1998**, *120*, 5343−5344.

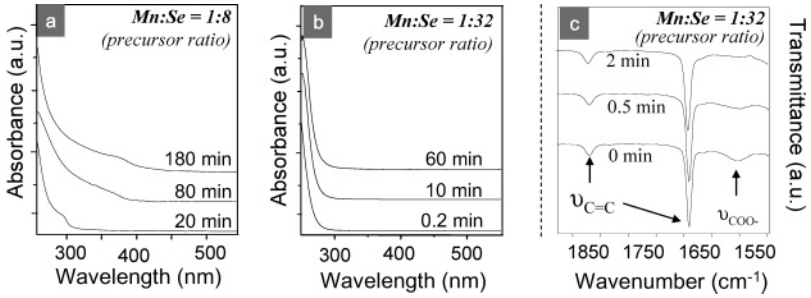

Figure 1. (a and b) Temporal evolution of the UV−vis spectra of the MnSe nanoparticles grown with different precursor ratios. (c) Temporal evolution of FTIR spectra for the case with Mn to Se precursor ratio being 1:32. The three IR peaks were assigned to C═C of ODE and the asymmetric stretching vibration of the $-COO^-$ group.

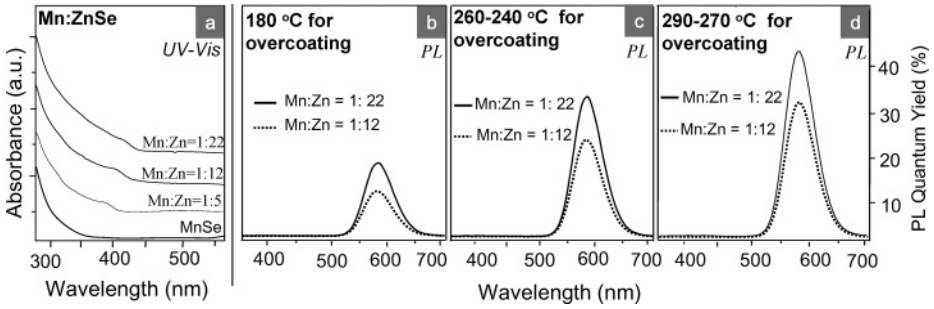

Figure 2. (a) UV−vis spectra of the d-dots in different growth stages. (b,c,d) PL spectra of the d-dots at different stages and different growth temperatures. The Mn:Zn ratio in each plot is the precursor ratio at a given growth stage. Excitation wavelength is 350 nm.

Figure S1). This brownish color was most likely associated with the formation of Mn hydroxide or oxide. The existence of such impurities made the formation of MnSe nanoclusters complicated and irreproducible, particularly when the Se concentration was low. Another issue related to the precursor was, if a significant amount of free fatty acid was not purified away, the formation of small-sized MnSe nanoclusters would become difficult because of the decreased reactivity of the metal carboxylate precursors as we observed previously.[30] It should be pointed out that the existence of free fatty acids could be easily detected using FTIR, with a carbonyl vibration peak between 1700 and 1720 cm^{-1}.

Overall, with the properly synthesized precursors and a relatively large excess of Se precursor, formation of small-sized MnSe nanoclusters was rapid (shorter than 10 min) and reproducible. The exact size of the excessively small MnSe nanoclusters could not be directly determined when using a transmission electron microscope (TEM). An indirect method will be discussed later.

The overcoating of ZnSe layer onto the MnSe particles was studied systematically by varying the reaction temperature for the overcoating process. Based on a general understanding of epitaxial growth,[31] the quality of the interface should be greatly influenced by the reaction temperature. However, the method reported in our previous communication was limited to 180 °C and with tributylphosphine as the coordinating solvent for limiting the reactivity of the zinc acetate precursor. It was expected that the composition of the reaction mixture must be significantly changed to increase the overcoating temperature. Because all overcoating processes were carried out in a one-pot fashion, meaning no isolation of the MnSe nanoparticles, the complete consumption of the Mn precursor and stability of the resulting MnSe nanoclusters were critically important, especially for the relatively high reaction temperatures to be discussed below. In this sense, a large excess of Se precursor for the formation of MnSe particles would be ideal.

All overcoating reactions were monitored with UV−vis spectroscopy. After each addition of zinc fatty acid salt precursor, the reaction was allowed to proceed until no observable changes were found by UV−vis within about 15 min intervals. Such a cycle, from the injection of zinc precursor to the completion of the ZnSe growth caused by the injection, is called a one growth step in this report. The final UV−vis spectrum after each growth step (Figure 2a) for the reaction carried out under different growth temperatures tested was about the same as long as the amount of zinc precursor injected was the same for a given growth step. Overall, the UV−vis spectra of the resulting d-dots are similar to those of quantum shell samples,[32] instead of quantum dots, as reported in the previous communication.[1] This is consistent with the structural feature of the core-doped d-dots, with the host semiconductor layer epitaxially grown onto the surface of the doped core particles. In fact, observation of sharp exciton absorption peaks similar to quantum dots was noted as a sign for the formation of undoped ZnSe nanocrystals.

PL QY of the resulting d-dots was found to be strongly dependent on the overcoating temperature (Figure 2b−d), although the UV−vis spectra for a given overcoating step were found to be almost independent of the growth temperature. Generally speaking, the higher was the overcoating reaction temperature, the higher was the PL QY (Figure 2). For the first growth step, however, the PL QY was generally low and not strongly temperature dependent (data not shown).

(30) Yu, W. W.; Peng, X. *Angew. Chem., Int. Ed.* **2002**, *41*, 2368−2371.
(31) Herman, M. A.; Sitter, H. *Molecular Beam Epitaxy: Fundamentals and Current Status, Second Revised and Updated Edition*; 1996; 453 pp.
(32) Battaglia, D.; Li Jack, J.; Wang, Y.; Peng, X. *Angew. Chem., Int. Ed. Engl.* **2003**, *42*, 5035−9.

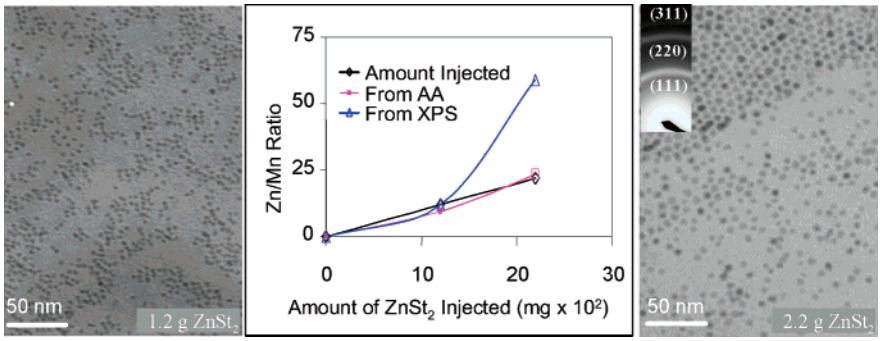

Figure 3. Zn to Mn ratio of d-dots and TEM images of the d-dots. The representative electron diffraction pattern of the d-dots is illustrated as the inset in the right plot.

It should be pointed out that d-dots with high PL QY, between 40% and 70%, could only be made with small MnSe nanoclusters and under relatively high overcoating temperatures. If the overcoating temperature was below 200 °C, the PL QY was found to be generally low, in the range between 10% and 30% for the highest values, similar to that reported in the previous communication.[1] In this temperature range, the size of the MnSe nanoparticles did not seem to make a definite difference. When the MnSe nanoparticles were the large-sized nanoparticles as shown in Figure 1b, the highest PL QY was found to be around 20−30%.

For all growth reactions, the PL QY of the d-dots increased significantly as the thickness of the ZnSe layer increased (Figure 2). As the ZnSe layer grew thicker, the emission centers, Mn ions, would be embedded deeper inside a d-dot and more isolated from the surface defects. Consequently, an enhanced PL QY should be the result.

Controlling the reactivity of zinc precursor was the key for boosting the overcoating reaction from 180 °C reported previously for the same type of d-dots[1] to 290 °C. The targeted reactivity of the zinc precursor should be sufficiently high to ensure the overcoating of the ZnSe layer, but low enough to avoid homogeneous nucleation of ZnSe nanocrystals. This balanced reactivity was achieved by using amines as activation reagents, tuning the chain length of the fatty acid salts, and adding free fatty acids as inhibitors. A brief discussion is offered below, and details can be found in the Experimental Section.

When zinc undecylenate ($ZnUet_2$) was used as the precursor, no free undecylenic acid (UeA) should be added if the overcoating temperature were chosen to be below 210 °C. Using the same precursor, UeA in a molar ratio to $ZnUet_2$ of 1:5 would be needed if the overcoating temperature were selected to be 240 °C. Even more UeA (molar ratio to $ZnUet_2$ being 2.5:1) would be necessary for a reaction with 260 °C as the overcoating temperature. $ZnSt_2$ has a longer hydrocarbon chain than does $ZnUet_2$, and reactions with $ZnSt_2$ as the precursor could thus be carried out under higher reaction temperatures with less corresponding free acid. Specially, for $ZnSt_2$-based reactions, the zinc precursor to stearic acid ratio was 5:1 for 260 °C, 2.5:1 for 290 °C, and 2:1 for 300 °C as the overcoating temperature. Other zinc carboxylates were also used for achieving desired overcoating temperatures. For example, zinc acetate was used for below 180 °C, and a zinc myristate/myristic acid mixture could be an option for overcoating temperature between 220 and 260 °C. Fatty amines were exploited as both ligands for the nanocrystals and for the activation reagents. However, a large excess of amine would sometimes cause the formation of

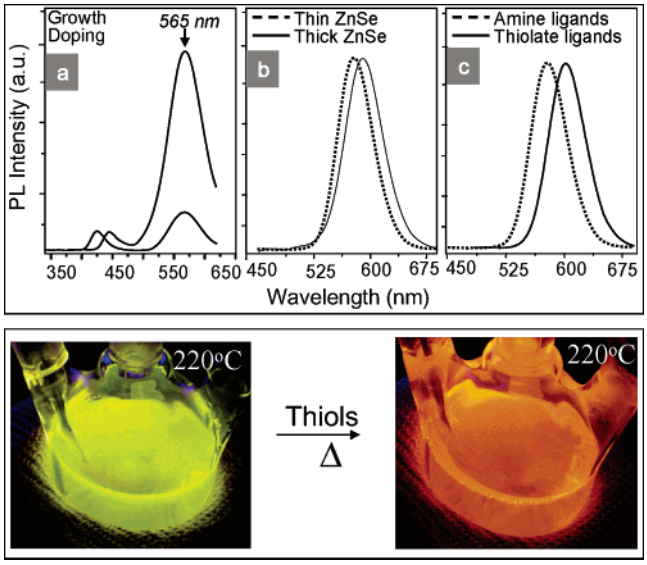

Figure 4. Top: Tunable emission peak position of d-dots grown under different conditions. Bottom: Color change upon the addition of thiol ligands.

ZnO[33] or ZnSe[34] nanoparticles, especially for the reactions at above 250 °C. Hence, periodical injections of amine were essential as the amines were consumed continuously (see details in Experimental Section).

In the previous communication,[1] tributylphosphine (TBP) was used for preventing the formation of pure ZnSe nanocrystals as mentioned above. The current system successfully eliminated the usage of TBP as a part of zinc precursor, and at the same time enabled a broad range of reaction temperatures.

The size and composition of the resulting d-dots were determined by TEM measurements, atomic absorption spectroscopy (AA), and X-ray photoelectron spectroscopy (XPS). For the samples used in the composition measurements in Figure 4, the average sizes of the d-dots were determined by the TEM images (Figure 3) as 4.3(±0.2) and 6.2(±0.3) nm, respectively. The d-dots for both samples were found to possess the same electron diffraction pattern that matched the pattern of zinc blende ZnSe nanocrystals, which is the same as what was reported in the previous communication.[1] This is structurally reasonable as MnSe can exist in zinc blende structures at the synthetic temperature (>180 °C). The lattice constants for the zinc blende MnSe and ZnSe are almost identical.

(33) Jana, N. R.; Chen, Y.; Peng, X. *Chem. Mater.* **2004**, *16*, 3931−3935.
(34) Li, L. S.; Pradhan, N.; Wang, Y.; Peng, X. *Nano Lett.* **2004**, *4*, 2261−2264.

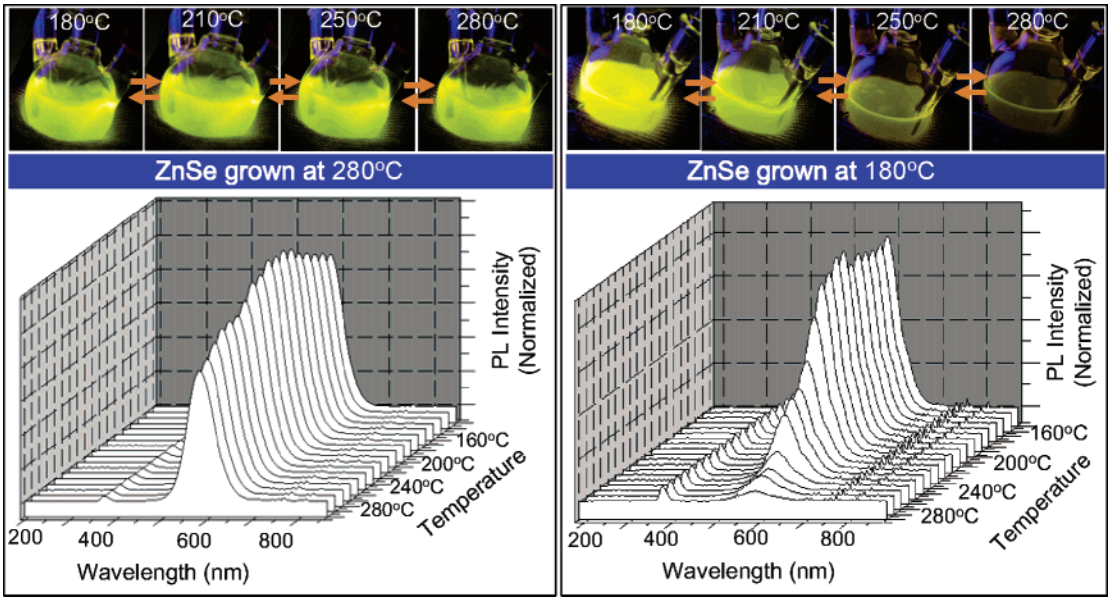

Figure 5. Thermal stability of PL of the d-dots grown with different overcoating temperatures. The peak at about 360 and the other small peaks beyond 700 nm are background noise.

The corresponding Mn to Zn ratio in the d-dots determined by AA followed the expected values calculated from the amounts of injected precursors (Figure 3). The Zn to Mn ratio of the smaller d-dots determined by XPS was slightly higher than that of the AA measurements. The Zn to Mn ratio of the larger d-dots determined by XPS, however, was found to be about 3 times higher than that from the AA measurements. This result is consistent with the targeted d-dot structure, with Mn ions located within the center of a d-dot. Because AA measurements provide the overall ratio of the two cations in a sample, so the observed Mn to Zn ratio should reflect the real value. However, XPS is mostly sensitive to the surface atoms.[35] As a result, it showed more Zn than the real value in a core/shell d-dot. For the same reason, the slightly higher Zn to Mn ratio for the d-dots formed by the low dose of zinc precursor implies that there was likely some interface diffusion between the preformed MnSe nanoclusters and the ZnSe coating layer for these small d-dots. This issue will be further discussed later.

By combining the sizing information obtained from TEM images of the d-dots and the Mn to Zn ratio determined by AA, one could actually calculate the size of the initial MnSe nanoclusters that were invisible under TEM. Assuming a spherical shape for both MnSe nanoclusters and the resulting d-dots, the obtained diameter of the initial MnSe nanocluster was estimated to be roughly around 1.5 nm. This value is consistent with the extremely high-energy absorption edge illustrated in Figure 1b.

The color tunability of the PL of Mn:ZnSe d-dots, from about 575 to 595 nm, was identified in the previous communication[1] as the thickness of the ZnSe shell increased. Our initial interpretation was that, as the ZnSe layer grew thicker, the lattice field around a given Mn center became more symmetric. As a result, the d-orbitals of the Mn center shall experience less electric field difference along different directions, which results in a smaller splitting of the energy levels.

If the above interpretation was reasonable, one would expect a significant red-shift of the PL spectra of a d-dot sample if their ligands were changed from a neutral species, such as aliphatic amines, to a charged one. Thiolate ligands, deprotonated thiols, are known as stronger ligands to II−VI semiconductor nanocrystals in comparison to amines.[36] Following this hypothesis, we added thiol ligands into the reaction mixture after the overcoating process was completed. Presumably, the added thiols shall be deprotonated to form thiolates by the excess amines existing in the reaction mixture.

Upon heating the reaction mixture with the thiolates at above 220 °C, the PL color of the d-dots in the reaction flask indeed changed gradually from bright yellow (PL peak at around 582 nm) to orange red (with a peak being around 610 nm) for the example in Figure 4 (bottom panel). The initial and final PL spectra of this treatment are shown in Figure 4c. Importantly, this treatment could stop at any moment and obtain a stable sample with a defined emission peak position, as long as there was no further thiol treatment. It should be pointed out that the thiol treatment process described here did not change the absorption properties of the d-dots.

However, the incorporation of sulfur anions into the d-dot lattice might also play a role for the red-shift observed with thiol ligands. As reported in literature, Mn:ZnS nanocrystals showed their PL peak at around 600 nm.[26] Furthermore, the red-shift of the PL peak observed with thiol ligands needed an excessively high temperature, above 220 °C as stated above. At such high temperature, decomposition of thiol ligands might have occurred.[37] Further studies, both theoretical modeling and experimental exploration are needed to definitely explain this interesting color tunability.

A preliminary experiment was carried out for Mn:ZnSe d-dots using the growth-doping strategy to see if there is any possibility to further tune the emission color of this d-dot system. As shown in Figure 4a, the dopant emission peak of the resulting d-dots

(35) Atkins, P. W. *Physical Chemistry*, 6th ed.; 1998; 1014 pp.
(36) Aldana, J.; Lavelle, N.; Wang, Y.; Peng, X. *J. Am. Chem. Soc.* **2005**, *127*, 2496−2504.
(37) Sigman, M. B., Jr.; Ghezelbash, A.; Hanrath, T.; Saunders, A. E.; Lee, F.; Korgel, B. A. *J. Am. Chem. Soc.* **2003**, *125*, 16050−16057.

was at about 565 nm, which was about 10 nm blue-shifted in comparison to the low limit for the corresponding d-dots synthesized using nucleation-doping. Unfortunately, we have not optimized the synthesis using the growth-doping strategy, and a small host emission was observed in the samples (Figure 4a).[17,24] The PL QY of these d-dots was quite low as well, not more than 10%.

Overall, efficient and pure dopant emission from Mn:ZnSe nanocrystals could be tuned from about 575 nm to about 610 nm (Figure 4). The green-yellow emission at about 565 nm from the growth-doping (Figure 4a) needs further optimization for practical applications. The overall tunable window was expanded to about twice as broad as the one reported in the early communication.[1]

Thermal stability of PL of d-dots is a key attractive feature for them to be considered as the next generation of nanocrystal emitters. Because of the strong coupling between excitons and lattice phonons for undoped quantum dots,[6] a strong thermal response has been considered as an intrinsic nature of their exciton emission. For this reason, the exciton emission of undoped quantum dots may not be ideal for high power applications, such as LEDs, solid-state lighting, and solid-state lasers, for which strong thermal effects are inevitable.

The PL of Mn:ZnSe d-dots grown by nucleation-doping strategy was found to be still bright up to about 220 °C in the previous communication.[1] This thermal stability is consistent with the nature of the emission states, which are inner core states (d orbitals split by the crystal field) and not coupled with the lattice phonons. Because of its importance, thermal stability of the d-dots synthesized using the new approaches discussed above was further studied in a more systematic and quantitative manner.

For the d-dots grown with an overcoating temperature at 280 °C, a slight increase of intensity from room temperature to 180 °C followed by a slight decrease for the further heating to 300 °C (Figure 5, left) was reproducibly observed by the PL spectra recorded in situ (see details in Experimental Section). Generally speaking, a PL intensity change within ±10% was observed in this temperature range. However, this intensity change was hardly visible by bare eye or the pictures taken by the digital camera (Figure 5, left) in the temperature range up to 300 °C (roughly the boiling point of the reaction mixture).

The d-dots grown with overcoating temperature at 180 °C (Figure 5, right), however, behaved quite differently. A dramatic decrease of PL brightness (in picture) or PL intensity (in PL spectra) was observed after the temperature increased beyond about 180 °C. Although the PL almost diminished at about 280 °C, it recovered reversibly if the d-dots were cooled down to 180 °C and below.

A close examination of the PL spectra at high temperature for the d-dots overcoated at different temperatures showed an interesting difference. As temperature increased, the contour of the PL spectra did not change for the d-dots overcoated at 280 °C, but the PL spectra for the d-dots overcoated at 180 °C became significantly asymmetric, with a visible shoulder at the high wavelength side (Figure 5). To better illustrate this difference, the PL spectra of the two samples at 250 °C were plotted together after normalization (Figure 6a).

Interestingly, if the overcoating process took place at an even lower temperature (150 °C), the PL QY was low (less than 10%)

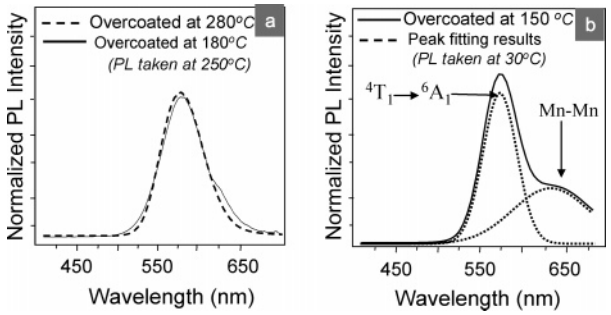

Figure 6. PL spectra of the d-dots overcoated with different temperatures.

and the low-energy shoulder became visible at room temperature (Figure 6b), which can be fitted into two PL peaks, one for the regular d−d transition (commonly called $^4T_1$ to $^6A_1$ transition)[13,38,39] and the other peak centered at about 640 nm. The 640 nm peak is similar to the PL peak position from the emission centers with a Mn ion next to the Mn emission center (Mn−Mn centers), instead of all zinc ions, observed in the bulk samples.[40] Such Mn−Mn emission centers, with a lower efficiency and shorter lifetime,[41] are different from the single emission center for the $^4T_1$ to $^6A_1$ transition. It should be pointed out that, because both transitions are optically not allowed, their extinction coefficients are extremely low. The UV−vis measurements with very high concentration of $MnSt_2$ and Mn:ZnSe nanocrystals, however, did show different absorption bands in the energy range expected for single Mn center and a mixed case, respectively (see Supporting Information, Figure S3).

Mn−Mn emission centers only occur when Mn dopant concentration was very high for bulk samples[40] and d-dots grown by traditional approaches.[41] However, the d-dots grown by nucleation-doping should have a great chance to possess such Mn−Mn emission centers because the Mn centers should be all from the central core in a d-dot in this specific case, and the Mn to host cation ratio was very high (Figure 3) as compared to typical doped semiconductors. More discussion on this issue will be given in the Discussion.

An interesting PL peak shift was observed upon thermal treatment of d-dots. The emission peak position of d-dots blue-shifted for about 5−8 nm reversibly by heating the solution from room temperature to about 300 °C. q-Dots, however, are known to red shift with the increase of temperature (Supporting information, Figure S5). At this moment, we do not have a reasonable explanation for this interesting phenomenon.

The PL peak width of an emissive material determines its color purity. Mn:ZnSe d-dots were always found to possess a full width at half-maximum (fwhm) around 52(±5) nm. This value is significantly broader than that of the exciton emission from high-quality CdSe quantum dots, around 22−25 nm fwhm,[42] in the similar optical window. However, the lifetime of dopant emission should be very long as reported in literature[43,44] and our own results (to be published separately) because the related transition is optically forbidden. Consequently, the intrinsic PL peak width for the dopant emission in

(38) Jones, G.; Woods, J. *J. Phys. D: Appl. Phys.* **1973**, *6*, 1640−51.
(39) Eno, E. E.; Grasser, R.; Scharmann, A. *J. Lumin.* **1981**, *24−25*, 261−4.
(40) Chen, W.; Sammynaiken, R.; Huang, Y.; Malm, J.-O.; Wallenberg, R.; Bovin, J.-O.; Zwiller, V.; Kotov, N. A. *J. Appl. Phys.* **2001**, *89*, 1120−1129.
(41) Suyver, J. F.; Wuister, S. F.; Kelly, J. J.; Meijerink, A. *Phys. Chem. Chem. Phys.* **2000**, *2*, 5445−5448.
(42) Qu, L.; Peng, X. *J. Am. Chem. Soc.* **2002**, *124*, 2049−2055.

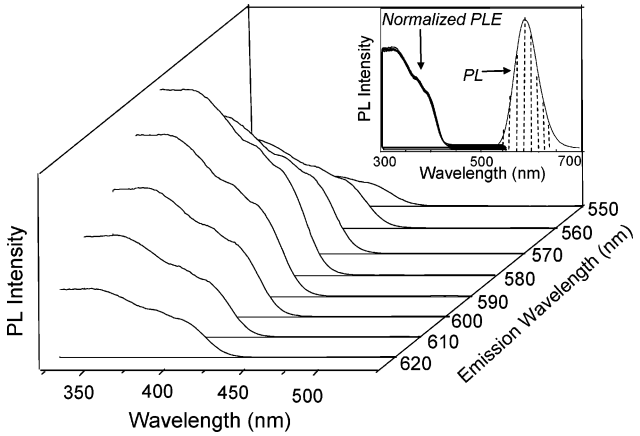

Figure 7. PLE spectra of the d-dots at different emission wavelengths. Inset: Normalized PLE spectra at different emission wavelengths, and each emission wavelength is indicated by a dashed line in the PL spectrum.

d-dots should be smaller, instead of larger, in comparison to that of the undoped quantum dots. This implies that the large fwhm for the d-dot PL is from inhomogeneous broadening.[45,46]

The inhomogeneous line width of the PL of undoped quantum dots can be revealed by photoluminescence excitation (PLE) studies if it comes from the size distribution of the corresponding nanocrystals. In principle, as the emission wavelength monitored in PLE shifts along the PL spectrum of a quantum dot sample from high energy to low energy, the PLE spectrum also shifts from high energy to low energy, if a broad PL peak width was caused by the size distribution.

To clarify the contribution of the size inhomogenity for PL peak width, PLE spectra of a d-dot sample were recorded at a set of emission wavelengths along the entire PL spectrum (Figure 7). Evidently, the intensity of the PLE spectra changed as the emission wavelength changed. However, the normalized PLE spectra were practically the same as shown in the inset in Figure 7. Therefore, it is reasonable to state that the emission at any wavelength was contributed from the entire ensemble of d-dots in a given sample. These results clearly indicate that, although the size distribution of the d-dots was not monodisperse (Figure 3), it did not contribute to the PL peak width.

Another type of commonly known spectral inhomogeneous line width is caused by the fluctuation and variation of the environment of emissive species. This is why the PL spectrum of an organic dye is often quite broad, and its PL position and width can change substantially upon simply changing its solvents, although an organic dye has a definite molecular structure. Likely, PL peak width of d-dots was also caused by the variation of the local environment of the Mn emission centers. Although the nucleation-doping chemistry demonstrated here has reached a reasonable degree of control, it was not difficult to imagine that a significant environment distribution for Mn emission centers was still in place. Single molecular spectroscopy experiments are planned to reveal the intrinsic line width of PL from d-dots, and further optimization of the synthetic chemistry will be also considered to explore possibilities for synthesizing d-dots, which are not only efficient, durable, and with zero self-quenching but also with a narrow emission line width.

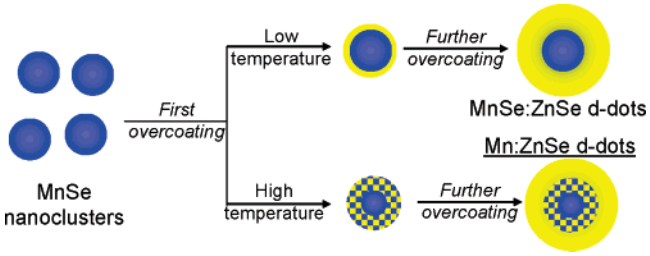

Figure 8. Schematic structures of the d-dots formed under different reaction temperatures.

Discussion

Although the main goal of this report is on developing synthetic chemistry of high performance d-dot emitters, some discussions on the structure of the resulting d-dots should help for understanding such composition engineered nanocrystals. At present, complete structural characterization of doped nanocrystals has not been reported. Needless to say, the key structural feature for a doped nanocrystal is the exact location and concentration of the dopant ions in a given nanocrystal, which may be partially assessable with those high-end X-ray absorption techniques. However, TEM, XPS, and AA results, along with spectroscopy data, including UV−vis, PL, and electron spin resonance, can provide some evidence to determine the structure of the d-dots.

Combining the XPS and AA measurements (Figure 3), one can conclude that the d-dots reported in this work did have a quasi core/shell structure, with the Mn ions mostly located close to the center of the structure. This is consistent with the targeted structure for nucleation-doping (Figure 8). There is some additional evidence to support such a core/shell structure. For instance, the increased PL QY (Figure 2) and improved chemical/photochemical stability (to be published separately)[27] of the d-dots upon the increase of the overcoating thickness are strong evidence to support the core/shell structures. Both sets of data indicate that the emission centers were becoming farther away from the surface as the thickness of the ZnSe coating layer increased. In addition, both absorption (Figure 2) and PLE (Figure 7) spectra of the d-dots were found to be similar to that of quantum shells,[32] instead of quantum dots. This implies that ZnSe likely formed a shell structure, instead of a uniformly mixed alloy with MnSe for the entire particle.

A core/shell structure indicates that the d-dots structures are significantly different from that grown by using doped nanoclusters as the precursors.[21] In the latter case, a large portion of the doped nanoclusters was destroyed and re-formed into large-sized doped nanocrystals probably through a ripening mechanism. In the nucleation-doping here, the nanoclusters acted as the nuclei for the growth of the host semiconductor.

The next question is how sharp the interface is between the MnSe core and ZnSe overcoating layer. The substantial PL signal from Mn−Mn emission center for the d-dots overcoated at 150 °C (Figure 6b) indicates that the integrity of the MnSe nanoclusters maintained reasonably well during the overcoating process at this low temperature. As the reaction temperature

(43) Bol, A. A.; Meijerink, A. *Phys. Rev. B: Condens. Matter Mater. Phys.* **1998**, *58*, R15997−R16000.
(44) Yan, K.; Duan, C.; Ma, Y.; Xia, S.; Krupa, J.-C. *Phys. Rev. B: Condens. Matter Mater. Phys.* **1998**, *58*, 13585−13589.
(45) Albe, V.; Jouanin, C.; Bertho, D. *Phys. Rev. B: Condens. Matter Mater. Phys.* **1998**, *57*, 8778−8781.
(46) Salvador, M. R.; Hines, M. A.; Scholes, G. D. *J. Chem. Phys.* **2003**, *118*, 9380−9388.

increased to above 280 °C, however, the Mn−Mn emission was decreased to a nondetectable level, and only a strong single Mn center emission was observed (Figure 6a). This implies that MnSe nanoclusters were less retained as the overcoating temperature increased, which indicates a diffused interface between the core and external shell. In other words, the exact structure of the Mn:ZnSe d-dots grown by nucleation-doping at a reasonably high temperature is unlikely a pure MnSe nanocluster core coated with a pure ZnSe shell. This diffusion, however, seems to be limited to a relatively thin ZnSe shell as indicated by the XPS results discussed above (Figure 3), the ligand modification experiments, and stability tests (to be published separately).[27] Figure 8 (bottom) provides a modified picture for the resulting Mn-doped ZnSe nanocrystals through nucleation-doping strategy, a $Mn_xZn_{1-x}Se$ core coated with pure ZnSe overcoating layer.

The reversible thermal response of the d-dots overcoated at 180 °C indicates that the diffusion process could not occur for the formed d-dots with a relatively thick ZnSe shell upon thermal annealing up to 300 °C. Instead, such diffusion should occur during the growth process. The reversibility along with the stability at a given temperature further imply that the d-dots structure formed in the temperature range studied here was thermally stable, without significant motion of the cations.

The picture suggested above (Figure 8) is important for the synthesis of high-quality d-dots through nucleation-doping and is thus worth to be further confirmed. Ideally, if the interface were the important region, the overcoating temperature for the first dose of zinc precursor would be important, at least more important than the following overcoating processes for thick ZnSe shells. The experimental results (Supporting Information, Figure S4) did confirm this prediction, that a higher temperature for the initial growth of ZnSe was indeed more important than a higher temperature for the subsequent overcoating for obtaining thermally more stable and more efficient d-dot emitters.

It is known that MnSe has a zinc blende structure identical to that of ZnSe. This metastable phase of MnSe was known to be stable above 180 °C. This is probably why we observed a maximum PL QY at 180 °C (Figure 5). The electron diffraction patterns of the resulting d-dots (Figure 3) were consistent with this common structure, and high-resolution TEM results revealed the single crystalline nature of the d-dots and did not show any crystal interface between the core and shell. It should be pointed out that MnSe was well known to be in zinc blende structure in an epitaxial system if the substrate was in zinc blend, such as GaAs.[47] In our case, MnSe was a small volume portion of the entire structure (Figure 3), and it is reasonable for MnSe to adopt a zinc blende structure. Furthermore, the pure $^4T_1$ to $^6A_1$ emission for the d-dots synthesized under a relatively high overcoating temperature (Figure 5) implies the Mn ion emission centers for these highly emissive d-dots are likely located on the common lattice positions and reasonably isolated from each other.

One may argue that the high PL QY and enhanced thermal stability of the d-dots grown under relatively high overcoating temperatures (Figures 2 and 5) was due to the high quality of the ZnSe shell formed at a higher temperature. At this moment, it is impossible to completely exclude the contribution from this possibility. However, it would be difficult to explain the disappearance of the Mn−Mn emission centers (Figure 6) just considering the structural imperfection of the ZnSe shell and without taking interface alloying into account. Furthermore, the PL QY of the d-dots with large-sized MnSe particles was found to be always low, below 30%, even when a high overcoating temperature was applied (see Results). This indicates that a high growth temperature alone, supposedly resulting in a better ZnSe shell, is not the sole determining factor for a high PL QY.

(47) Eunsoon, O. h.; et al. *Phys. Rev. B* **1993**, *47*, 7288.

Conclusion

In conclusion, synthesis of highly efficient (40−70% PL QY) and thermally ultrastable (up to boiling point of the solvent, 300 °C) Mn:ZnSe d-dots was studied systematically using greener approaches by nucleation-doping strategy. The main discovery of the current work, in comparison to the existing report,[1] is that small size of the MnSe nanoclusters (about 1.5 nm) and a diffused interface between MnSe core and ZnSe shell were identified as two key parameters for obtaining the high-quality d-dots. Furthermore, methods were developed to satisfy these two key parameters by optimizing nucleation temperature, overcoating temperature, structure of the precursor, and composition of reaction solutions at different stages. d-Dots synthesized under optimized conditions were found to be extremely thermally stable, up to the boiling point of the solvent (around 300 °C), which was quantitatively verified by in-situ measurements. The tunability of the PL color of the Mn:ZnSe d-dots was expanded to a quite broad window, from 565 to 610 nm. The emission color purity of the d-dots, the PL peak width, was identified not to be related to the size distribution of the d-dots. Applications[27] of d-dots as biological labeling reagents and lighting devices offered encouraging evidence for exploiting these non-heavy metal-containing nanocrystals as practical emissive materials.

Experimental Section

Materials. Zinc stearate ($ZnSt_2$, 12.5−14% ZnO), stearic acid (SA, 95%), selenium powder (~200 mesh, 99.999%), tetramethylammonium hydroxide pentahydrate (TMAH), manganese chloride ($MnCl_2$), dodecanethiol (DDT), and octadecylamine (ODA, 95%) were purchased from Alpha Aesar. 1-Octadecene (ODE), mercaptopropionic acid (MPA), and tributyl phosphine (TBP, 95%) were purchased from Aldrich. Zinc undecylenate ($ZnUet_2$) was purchased from Gelest. Undecylenoic acid (UeA) was purchased from TCI, and Rhodamine 3B dye was purchased from Eastman. All chemicals were used without further purification.

Synthesis of Manganese Stearate ($MnSt_2$). (A) In a typical synthesis, SA (20 mmol) was dissolved in 30 g of methanol and heated to 50−60 °C, or sonicated, until it became a clear solution and was then allowed to cool to room temperature. The solution of TMAH was prepared by taking 20 mmol of TMAH in 10 g of methanol and mixing with the SA solution. The mixture was stirred for 15 min to ensure the reaction had gone to completion. To this solution, 10 mmol of $MnCl_2$ dissolved in 10 g of methanol was added dropwise with vigorous stirring, and a white precipitate of $MnSt_2$ slowly flocculated. The precipitates were repeatedly washed with methanol and dried under vacuum. (B) Alternatively, $MnSt_2$ was also prepared by mixing SA and $MnCl_2$ solution together in a 2:1 molar ratio, and the base, TMAH, was added dropwise to obtain a brownish precipitate of $MnSt_2$. Digital pictures of the two types of synthesized $MnSt_2$ are shown in Figure S1.

Preparation of Stock Solutions. TBPSe solution was prepared inside a Glovebox by adding 1.9 g of Se to 8 g of TBP. Several types of zinc precursor solutions were prepared according to the type of

zinc carboxylate salt used. For example, when $ZnUet_2$ was used, the zinc precursor solution was prepared by mixing 1.9 g of $ZnUet_2$ and 0.6 g of UeA into 8 g of ODE. For the case of $ZnSt_2$, $ZnSt_2$ (1.8 g) and 0.4 g of SA were dissolved into 7 g of ODE. The amount of free acid for each was varied depending on the injection temperature as described in the text.

(A) Typical Synthesis of d-Dots. ODE (25 mL) and 0.1 g of $MnSt_2$ were loaded into a 100 mL three neck flask and degassed at 100 °C for 20 min by bubbling with argon. The temperature was then raised to 280 °C. In a separate vial, ODA (1 g) and 1 mL of TBPSe stock solution were mixed and heated to ∼70 °C, and injected into the above reaction flask at 280 °C. After the injection, the color of the solution rapidly turned faint yellow, which indicated formation of MnSe nanoclusters. The reaction was cooled to 260 °C and annealed for 60 min. The reaction temperature was then set at 240 °C (or another designated overcoating temperature) for ZnSe overcoating. Next, heated $ZnUet_2$ stock solution in ODE (3 mL) was injected into the reaction flask. Immediately after the $ZnUet_2$ injection, the solution started to glow yellow under UV-light, showing the growth of ZnSe on MnSe nanoclusters. The temperature was further cooled to 230 °C, and 0.5 g of heated ODA in 0.5 g of ODE was injected into the reaction mixture to activate the zinc carboxylates. The remaining $ZnUet_2$ stock solution was injected by adding 3 mL after 15 min intervals, followed by ODE/ODA injection. The growth process was monitored through successive UV−vis and PL measurements. Finally, the reaction was cooled to room temperature, and the nanocrystals were precipitated using acetone. Nanocrystals (about 200 mg) produced using this procedure were reproducible, demonstrating 25−40% QYs. If the overcoating temperature was set as 250 °C with calculated amounts of $ZnUet_2$ and UeA, the resulting d-dots typically had 30−45% QYs.

(B) d-Dots Formed by High Overcoating Temperature. To reduce the possibility of forming pure ZnSe particles, free acids were mixed with zinc precursors as inhibitors. Periodic introduction of amines as discussed in the above paragraph must be performed to avoid accumulation of excess free acid introduced by the injections, which maintained a reasonable reactivity for the zinc fatty acid/salt fatty acid mixture in the reaction solution.

Formation of MnSe nanoclusters was performed according to the procedure discussed in section A. After the MnSe solution was annealed at 260 °C for 60 min, the reaction temperature was increased to 290 °C for overcoating of ZnSe. The zinc precursor solution was prepared by dissolving 2 g of zinc stearate and 0.4 g of stearic acid into 8 g of ODE. This solution was maintained warm using a heat-gun, degassed with argon, and injected into the reaction flask, in 3 mL/15 min intervals as discussed above, which was set at 290 °C. Immediately after the injection, the reaction mixture was able to emit bright yellow under UV-light. The reaction was cooled down to 260 °C, and 0.5 g of ODA in 0.5 g of ODE was injected into the reaction mixture to maintain the amine concentration. Other procedures were similar to the ones described in section A. The resulting d-dots had a measured QY of 35−55%. The fwhm of the emission peak was 52(±2) nm for both systems.

(C) Tunable d-Dot Emission from ∼580 to ∼610 nm. For any of the aforementioned reaction systems, the emission peak position can be tuned by the addition of thiol. To maintain a high PL QY, the thickness of the ZnSe layer must reach a reasonable thickness, with its absorption band-edge beyond 440 nm, before the addition of the thiol. Injection of the thiol was performed at a temperature above 220 °C. For a reaction with 12 g of ODE, 2 g of ODA, 0.03 g of $MnSt_2$, and 0.5 g of $ZnSt_2$, nearly 2 g of dodecanethiol was injected. After the thiol injection, the reaction was allowed to continue until the PL peak position shifted from about 580 nm to a designated wavelength, but not beyond 610 nm. For a reaction in a 50 mL reaction flask, it took about an hour for the emission to shift to 610 nm at 260 °C. The reaction was monitored by UV−vis and PL measurements. During this process, the UV−vis spectra remained unaltered, although the PL position shifted from ∼580 to 610 nm.

Optical Measurements. UV−vis spectra were recorded on an HP 8453 UV−visible spectrophotometer. Photoluminescence spectra were taken using a Spex Fluorolog-3 fluorometer. The PL QY was measured following a suggested protocol in the manual of the Fluorolog-3 (see Supporting Information). Infrared spectra were obtained on a Bruker Tensor 27 spectrophotometer. IR samples were prepared by dropping hot aliquots directly taken from the reaction solution onto a NaCl disc. X-ray photoelectron spectra (XPS) were recorded using a Kratos Axis HSI spectrometer. Samples were prepared by dropping purified d-dot solution onto platinum films. Atomic absorption (AA) measurements were carried out using a GBC 932 Plus spectrophotometer after digesting the samples in concentrated nitric acid.

In Situ Measurements. Photoluminescence of d-dots at high temperature was measured directly from the reaction flask using an Ocean Optics USB 2000 spectrophotometer. Positions of the UV-source and fiber optic probe were fixed throughout the measurements. Successive photoluminescence spectra were recorded during cooling and heating of the reaction system from 290 to 100 °C and vice versa.

Transmission Electron Microscopy (TEM). TEM images were taken on a JEOL X-100 electron microscope using a 100 kV accelerating current at 50k magnification. Specimens were prepared by dipping a Formvar-coated copper grid into a toluene solution of the nanocrystals, and the grid with the nanocrystals was dried in air. Selected area electron diffraction pattern (SAED) was taken with a camera length of 120 cm.

Acknowledgment. Financial support of this work was provided by the National Science Foundation. Synthesis of Mn fatty acid salt precursors was developed by Dr. Yongfen Chen in Peng's research group. Discussions with David Battaglia at NN-Labs are also acknowledged.

Supporting Information Available: Supporting results mentioned in the text. This material is available free of charge via the Internet at http://pubs.acs.org.

JA068360V

Supporting Information

Efficient and Color-Tunable Mn-Doped ZnSe Nanocrystal Emitters: Control of Optical Performance via Greener Synthetic Chemistry

Narayan Pradhan and Xiaogang Peng*

Department of Chemistry & Biochemistry, University of Arkansas, Fayetteville, AR-72701

Email: xpeng@uark.edu

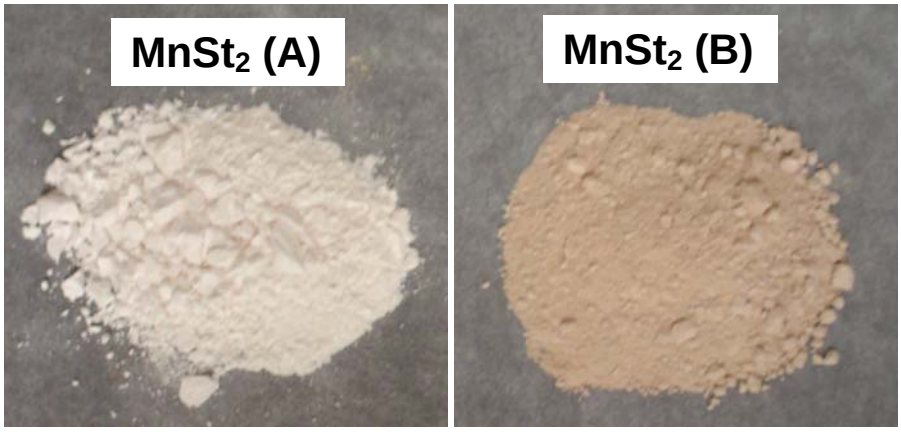

Figure S1. Digital pictures of manganese stearate ($MnSt_2$) synthesized using two different processes. Left one (A) is synthesized first neutralizing stearic acid with tetramethyl ammonium hydroxide and then $MnCl_2$ solution is dropwise added. Right one (B) is prepared by mixing $MnCl_2$ and SA, and base TMAH is added dropwise to get the precipitate.

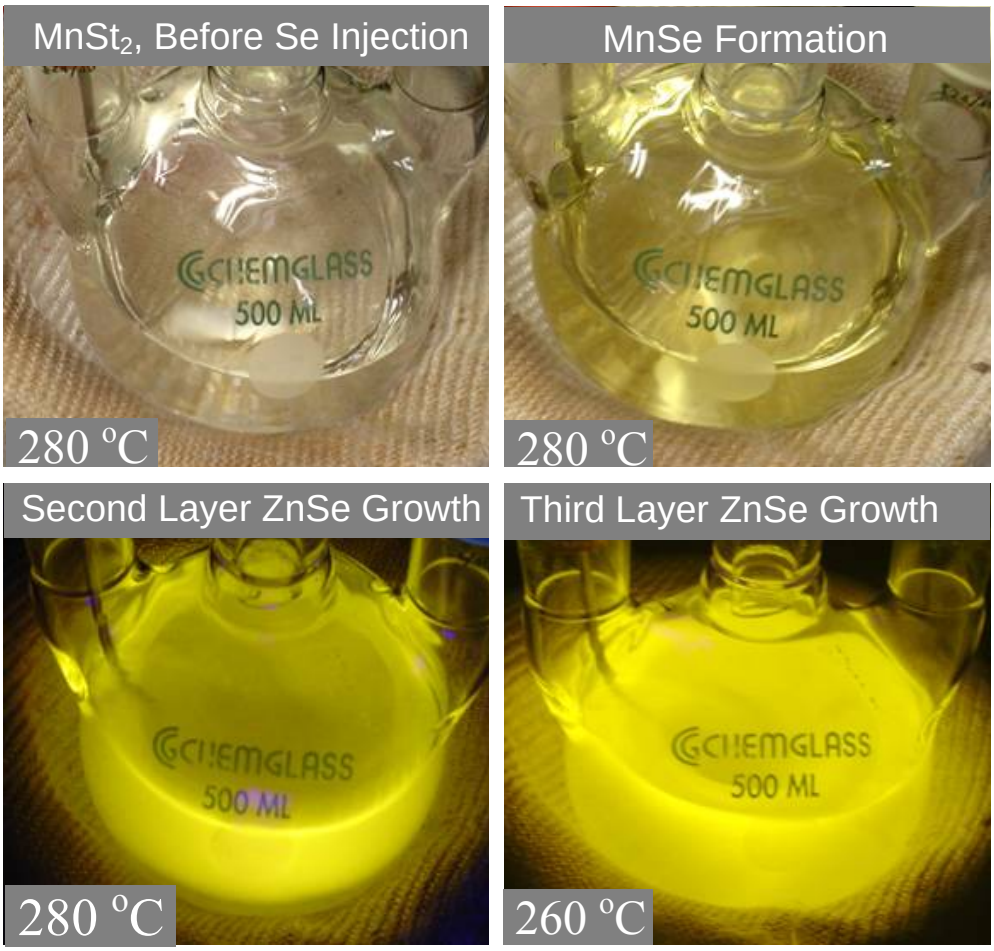

Figure S2. Digital pictures taken from the reaction flask at different stages. Bottom pictures are taken using a hand held UV-lamp irradiation.

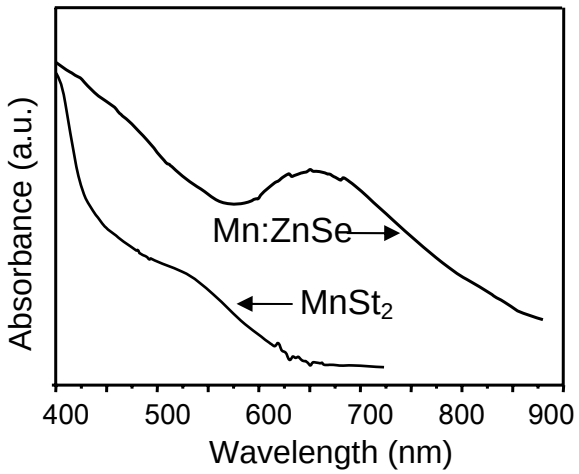

Figure S3. Absorption spectra of $MnSt_2$, and Zn:MnSe at very high concentration, directly taken from the reaction flask.

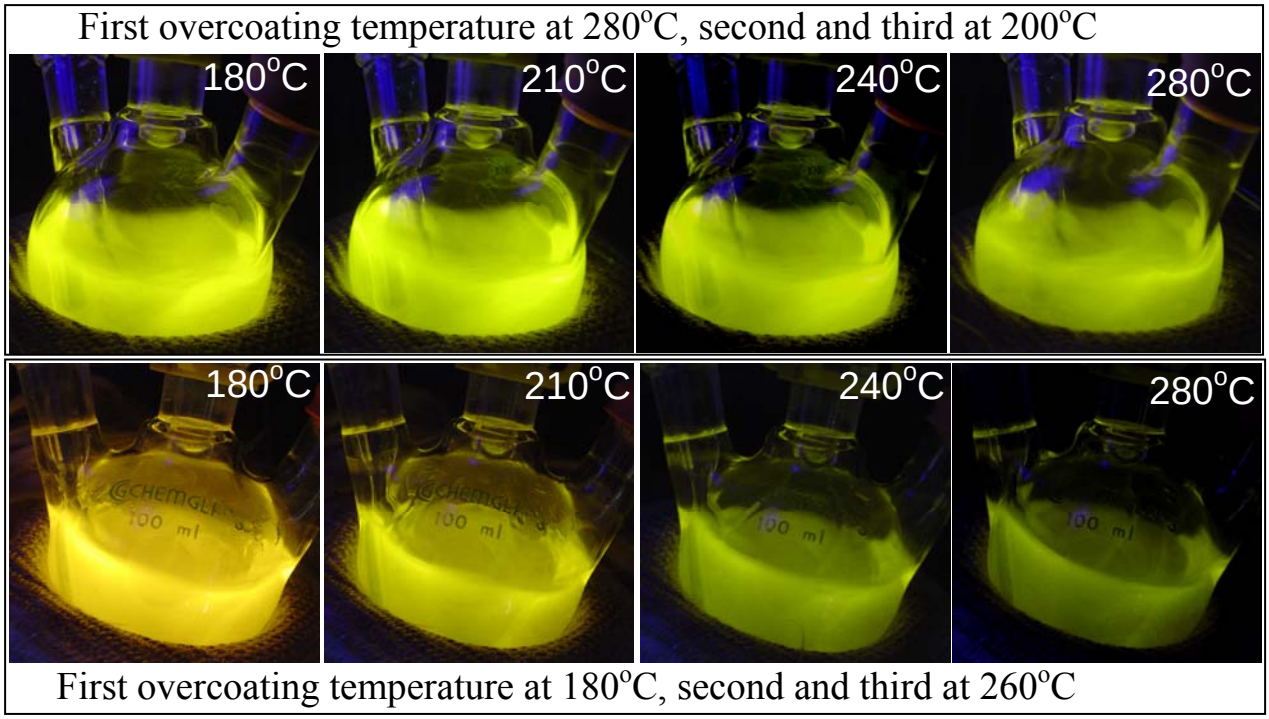

Figure S4. Digital pictures taken during heating of two set of reactions; Top panel is synthesized with the first injection at 280 °C and the rest growth at 200 °C, and bottom panel has 200 °C as the first injection and 260 °C for the rest of the ZnSe growth.

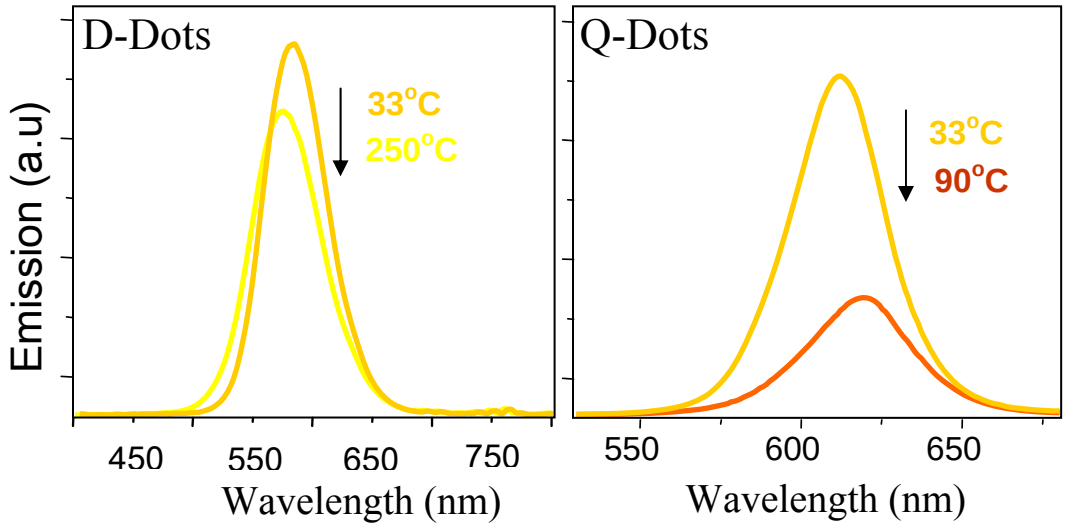

Figure S5. Photoluminescence change of Mn:ZnSe (d-dots, left) and CdSe (q-dots, right) with increase of temperature. It is blue shifted for d-dots and red shifted for q-dots.

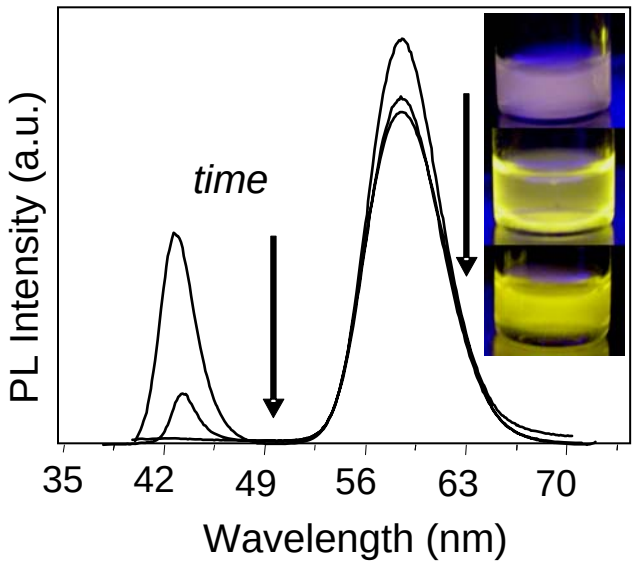

Figure S6. Mn doped (right peak) and undoped (left peak) ZnSe NCs mixed together in pyridine. Undoped nanocrysals quenches the luminescence within seconds but dopant emission retained. Inserts are the digital pictures taken during mixing pyridine into the nanocrystal solution.

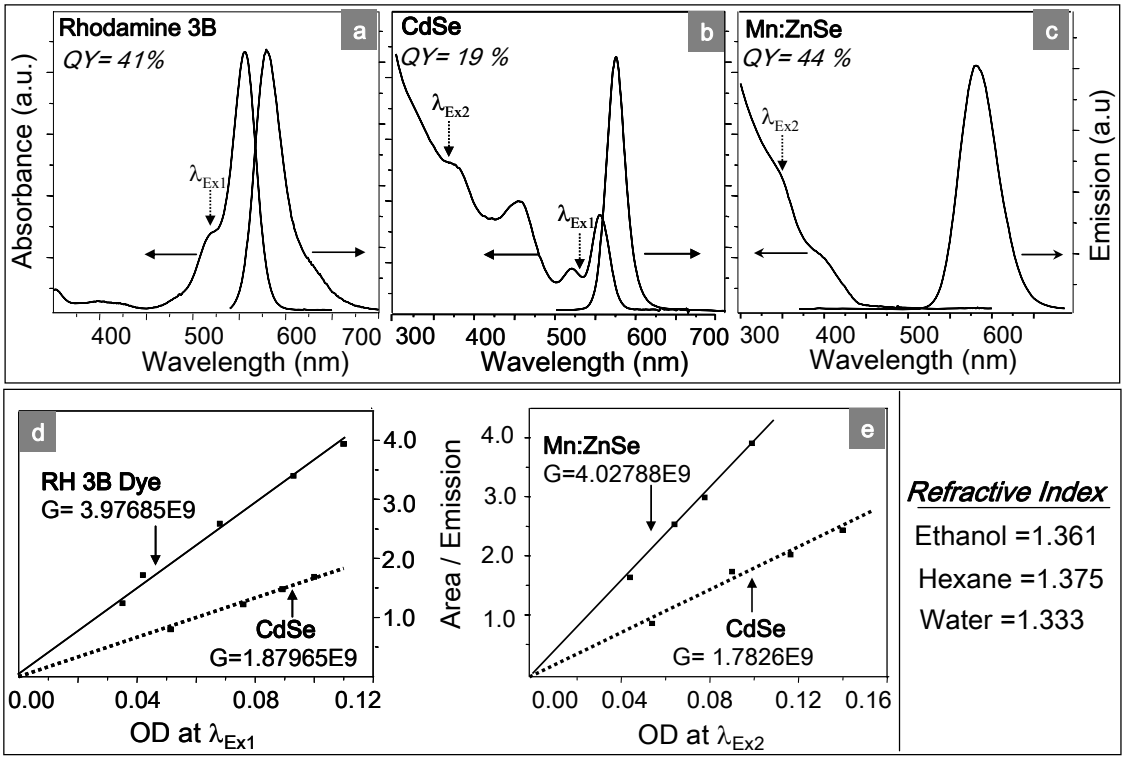

Figure S7. Top panel: UV-Vis and PL spectra of Rhodamine 3B (RH 3B) (a), CdSe dots (b), and Mn:ZnSe d-dots (c). Bottom Panel: Determination of PL QY for CdSe dots (d) and d-dots (e).

The PL QY measurements of d-dots are more complicated than that for undoped quantum dots. This is so because, at present, PL QY of nanocrystals has been measured using a reference organic dye with known PL QY. To reduce the error, a suited reference dye should have an overlapping emission peak with that of the nanocrystals and can be exited at the same wavelength. However, it is not easy to find a reference dye for d-dots due to their unusually large Stokes shift (Figure 7s, top panel). To solve this problem, we used CdSe quantum dots as the intermediate reference (Figure 7s).

It should be pointed out that this protocol is suggested in the instrument manual by the instrument manufacture. The PL QY of d-dots were also measured using a simple organic dye, as it was done in literature (ref 17), and the obtained values were within 10% error.

The PL QY of the CdSe dots sample was determined by using Rhodamine 3B (RH 3B) dye as the reference, both of which could be excited using the first excitation wavelength (λ_{ex1}). In the second step, the PL QY of a d-dots sample was measured by using the calibrated CdSe dot sample as the reference, again with the same excitation wavelength (λ_{ex2}) that was at a relatively high energy wavelength in comparison to the first excitation wavelength (λ_{ex1}). The emission window of the three samples, the dye, the CdSe q-dots, and the d-dots, overlapped with each other. The PL QY can thus be calculated using the traditional method. This method requires that the PL QY of CdSe nanocrystals must be the same at two different excitation wavelength. Fortunately, the CdSe quantum dots used in this work do have such feature (see Qu & Peng, JACS 2002, vol 124, 2049)

The PL QY measured using this method was further confirmed by a protocol suggested in the manual of the fluorometer used in our experiment. Multiple concentrations were examined for each sample and the data were plotted in Figure 7s (Bottom panel). The data for a given sample with a given excitation wavelength but with different concentrations should fit nicely in a linear line that must go through the origin. The PL QY of a testing sample was subsequently calculated from the slope of the line, the refraction index of the solvents, and the PL QY of the standard using the following equation.

$$QY_{dots} = QY_{REF} \times \frac{Slope_{dots}}{Slope_{REF}} \times \frac{(RI_{REF})^2}{(RI_{dots})^2}$$

REF = Reference (Dye or CdSe q-dots), dots = nanocrystals (q-dots or d-dots), RI = refractive index of a solvent.